Electromagnetic Field and Force Analysis of Three-Phase Enclosure Type GIS Bus Capsule

Xiangyu Guan and Naiqiu Shu

Department of Electrical Engineering
Wuhan University, Wuhan 430072, China
Xiangyuguan1986@163.com, shunaiqiu@21.cn

Abstract **─** With the aim to optimization design and condition monitoring of Gas Insulation Station (GIS), a 3-D finite element model has been developed for the computation of the electromagnetic field and forces in a three-phase enclosure type GIS bus capsule. The calculation takes into account the bus bar connectors' contact resistance by modeling equivalent contact bridges between contact interfaces and physical properties of the materials involved have also been considered. Using the field distributions, power losses and electromagnetic forces have been calculated, the calculation is more valid and accurate compared to those from closed-formulas. The influence of the operation current and short current on those quantities is also examined. The results show that the distributions of current density and electromagnetic force in the conductors and tank are not uniform. Electromagnetic force of plug-in connector obtained by closed-formulas calculation has obvious deviation, due to the current distributions are not considered. The electromagnetic forces of bus conductors and plug-in connectors are large enough to overcome hold forces exerted by the contact springs under short circuit conditions.

Index Terms **─** Eddy currents, electromagnetic forces, finite element methods, GIS, plug-in connector, power loss and short circuit.

I. INTRODUCTION

Gas Insulation Substation (GIS) has been widely used in modern power system for its land saving and high reliability. Three-phase enclosure type GIS bus capsule has been extended in higher voltage GIS, because of its advantage in minimizing the installation space of a substation [1]. Since all parts have been sealed inside the metal tank and the short distance between bus conductors, temperature rise and mechanical strength of bus connectors and tank joints under normal and short circuit currents are key problems in GIS design and maintenance.

The 2-D finite element model has been used to solve problems concerning electromagnetic field and temperature rise of GIS bus and SF_6 insulated cables [2-4]. The uneven distribution of current density in GIS bus conductor due to the skin effect and proximity effect is proposed [5]. The electromagnetic forces in different devices are calculated by 3-D finite element method [6-9]. The characteristics of short circuit forces and electromagnetic oscillations of three-phase enclosure type GIB based on experiments and method of image are proposed [10-12]; analysis results show that the characteristics of short circuit electromagnetic forces in three-phase GIB are notably different from those in single phase bus bars and the fundamental mode of conductor oscillation is dominant. Taking into account of skin effect, a more accurate calculation model of 3-D nonlinear transient electromagnetic forces in a three-phase enclosure type GIB is proposed [13]. However, although the fact that plug-in connectors' power loss and electromagnetic forces are important in designing equipment, existing calculation models of GIS cannot take into account the plug-in connector. The power loss of bus connector may cause contact temperature rise. All the parts of the device should be able to withstand the short circuit electromagnetic force.

In this paper, a 3-D finite element model of three-phase enclosure type GIS bar capsule has

Submitted On: January 9, 2014
Accepted On: July 19, 2014

been developed. The geometric model is shown in Fig. 1. The fingers fixed with springs are used to connect the bus bar plug and disc-type insulator and the shields can ensure uniform distribution of electric field. The assumptions about the calculation model are as follows:

1. The operation current frequency is 50 Hz and the calculation model is based on quasi-static approximation.
2. The variation of electric field cannot influence magnetic field. To simply matters, some parts chamfers, which used to improve electric field are neglected.
3. Contact force is constant and the springs of connector are neglected.
4. The roughness of contact interface is neglected and mechanical contact happens on one equivalent contact spot.
5. The nonlinearity of the material and displacement currents are neglected.

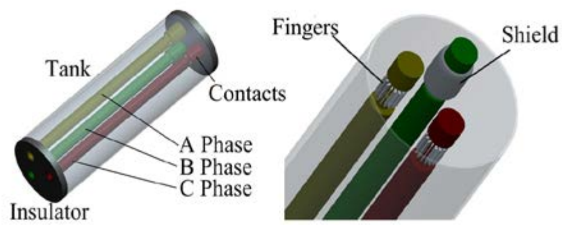

Fig. 1. Schematic structure of a three-phase enclosure type GIS bus bar capsule.

II. FORMULATIONS

A. Electromagnetic field equations

Since steady state ac flows in the bus conductor, the quasi-static approximation can be used.

In terms of the magnetic vector potential **A**, the Maxwell's equations can be rewritten as:

$$\left.\begin{aligned}\nabla\times\mathbf{H}&=\mathbf{J}\\ \nabla\times\mathbf{E}&=-\frac{\partial\mathbf{B}}{\partial t}\\ \mathbf{B}&=\nabla\times\mathbf{A}\end{aligned}\right\}. \tag{1}$$

The governing equation (2) can be derived as:

$$\nabla\times\mu(\nabla\times\mathbf{A})=\mathbf{J}\,, \tag{2}$$

where μ is the magnetic permittivity.

Using the vector equation (3) and the Coulomb's gauge (4), the governing equation (2) can be written as the Poisson's equation (5):

$$\nabla\times(\nabla\times\mathbf{A})=\nabla(\nabla\cdot\mathbf{A})-\nabla^2\mathbf{A}\,, \tag{3}$$

$$\nabla\cdot\mathbf{A}=0\,, \tag{4}$$

$$\nabla^2\mathbf{A}=-\mu\mathbf{J}\,, \tag{5}$$

where the total current **J** consists of the source current $\mathbf{J_s}$ and the eddy current $\mathbf{J_e}$:

$$\mathbf{J}=\mathbf{J_s}+\mathbf{J_e}. \tag{6}$$

The eddy current $\mathbf{J_e}$ in conducting material can be written as:

$$\mathbf{J_e}=\sigma\mathbf{E}=-\sigma\frac{\partial\mathbf{A}}{\partial t}\,, \tag{7}$$

where σ is the electrical conductivity.

B. Solution regions and boundary conditions

One cross section of GIS capsule is shown in Fig. 2, which represents the solution region. Eddy currents in the tank and shields are induced by the time varying source currents that flow through the main conductor. The tank surrounded by air is filled with SF_6 gas.

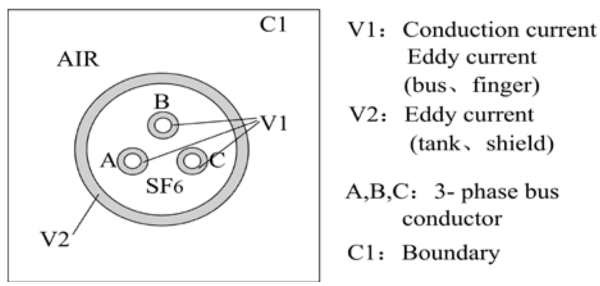

Fig. 2. Solution regions and boundary conditions.

Since 50-Hz ac flows through the bus conductor, the governing equations of different solution regions are written as:

$$\nabla^2\dot{\mathbf{A}}=j\omega\mu\sigma\dot{\mathbf{A}}-\mu\dot{\mathbf{J}}_\mathbf{s}. \quad \text{in } V_1, \tag{8}$$

$$\nabla^2\dot{\mathbf{A}}=j\omega\mu\sigma\dot{\mathbf{A}}. \quad \text{in } V_2, \tag{9}$$

$$\nabla^2\dot{\mathbf{A}}=0. \quad \text{in } SF_6 \text{ and AIR}. \tag{10}$$

The boundary conditions are as follows

$$\dot{\mathbf{A}}\Big|_{C1}=0\,, \tag{11}$$

$$\left.\begin{aligned}&\dot{\mathbf{A}}_\mathbf{1}=\dot{\mathbf{A}}_\mathbf{2}\\ &\mu_1\nabla\times\dot{\mathbf{A}}_\mathbf{1}\cdot n_{12}=\mu_2\nabla\times\dot{\mathbf{A}}_\mathbf{2}\cdot n_{12}\\ &n\cdot(-j\omega\varepsilon\dot{\mathbf{A}}-\varepsilon\nabla\dot{\phi})=0\end{aligned}\right\} \quad \text{in } S, \tag{12}$$

where S is the boundary of conductor material (V_1 and V_2) and no current regions (SF_6 and air), ε is the electric constant.

C. Contact bridge model

According to the Holm electric contact theory, when the conductor current flows through contact interface, the contact resistance and the electromagnetic repulsion force between bus connectors are induced by the constriction effect of current. A contact bridge model between finger and bus plug has been developed in order to simulate this constriction effect. The height of contact bridge is 0.2 mm and the radius of contact bridge can be calculated as the Hertz formula:

$$a = (3F_j R / 4E^*)^{1/3}, \tag{13}$$

where a is the contact bridge radius, F_j is the contact force, R is the equivalent radius of contact finger and conductor plug, E^* is the equivalent Young's modulus of fingers and conductor plug. All these parameters can be obtained from special GIS bus bar capsule design.

The per finger contact force of plug-in connector exerted by three circular holding springs can be calculated as:

$$F_j = 3K\pi^2 (D_1 - D_0) / n, \tag{14}$$

where K is the spring stiffness coefficient, π is the circular constant, n is the number of fingers and n=16, D_0 and D_1 are the diameters of the spring center line before and after loading. respectively.

D. Power losses

The power loss P generated by the joule heat is expressed as:

$$P = \int_V \frac{|\mathbf{J}|^2}{\sigma}. \tag{15}$$

The additional power loss P_a on the contact interface produced by contact resistance is written as:

$$P_a = |\mathbf{J_f}|^2 R_j, \tag{16}$$

where $\mathbf{J_f}$ is the current of per finger, R_j is the contact resistance which contains constriction resistance and film resistance; in this calculation the film resistance can be neglected since the chemical property of SF_6 is very stable under the working temperature of GIS. The constriction resistance R_c can be calculated by:

$$R_c = \rho / 2a, \tag{17}$$

where ρ is the resistivity of connectors and a is the radius of contact bridge.

E. Electromagnetic forces

Enclosure current is induced by the alternating magnetic field produced by conductor current. Electromagnetic forces are created by the interaction between current carriers and alternating magnetic field. The electromagnetic force act on current carriers can be expressed as:

$$\mathbf{F} = \int_V \mathbf{J} \times \mathbf{B} dV. \tag{18}$$

Electromagnetic forces of conductors are influenced by the tank current, the magnetic flux in the tank and the currents in other phase conductors. A image currents method is used to calculate the short circuit electromagnetic force in three phase enclosure type GIB [10].

Plug-in connector used in GIS bus connection belongs to static contact without switch operation. The electromagnetic force on the plug-in connector consists of the Holm force F_H and the Lorentz force F_L, which can be written as:

$$F_H = \frac{\mu_0}{4\pi} i_1^2 \ln\left(\frac{R}{a}\right), \tag{19}$$

$$F_L = K_c K_f \frac{\mu_0}{4\pi} i_2^2, \tag{20}$$

where μ_0 is the permeability of vacuum, i_1 and i_2 are currents in the plug-in connector and conductor, K_c is the loop coefficient and K_f is the conductor form factor.

III. CALCULATION MODEL

A 3-D FEM model of three-phase enclosure-type 110kV GIS bus bar capsule has been developed for the power loss and short circuit electromagnetic force calculation. The material and geometrical properties are shown in Table 1. The mesh of solution region is shown in Fig. 3. The initial contact force between each contact spot is 37N and the contact resistance is 57μΩ.

Table 1: Simulation model parameters

Tank Material	Aluminum alloy 6063-T6
Finger Material	Copper T2Y
Shield Material	Aluminum alloy 6063-T6
Bus Material	Aluminum alloy 6063-T6
Insulator Material	Epoxy resin
Tank Size	Φ596/Φ580
Bus Size	Φ90/Φ60
Span	2300mm

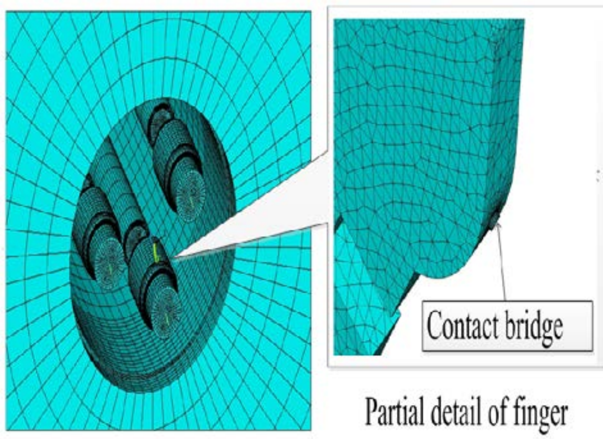

Fig. 3. Mesh of solution region.

IV. STEADY ELECTROMAGNETIC FIELD ANALYSIS

A. Steady state electromagnetic field analysis

The magnetic flux and current density distributions in the conductors and tank under normal load current (2000A) are shown in Fig. 4, and the current density distributions in the B phase plug-in connector are shown in Fig. 5. It can be seen from field distribution results that the current distributions in the bus conductors and tank are not uniform, because of skin effect and proximity effect. Due to the constriction effect of current line between plug-in connector and conductors, the current densities in contact spots are significantly larger than those in other parts and the individual finger contact spot temperature will rise higher, owing to the large current density. Uneven distribution of current density will cause uneven distribution of power loss and temperature rise in the three-phase enclosure type GIS bus capsule. Bus bar and tank flange connectors should be able to withstand the thermal stress caused by non-uniform temperature distribution for a long time.

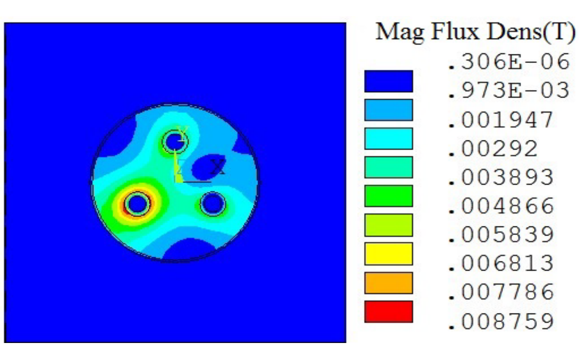

(a) Magnetic field density

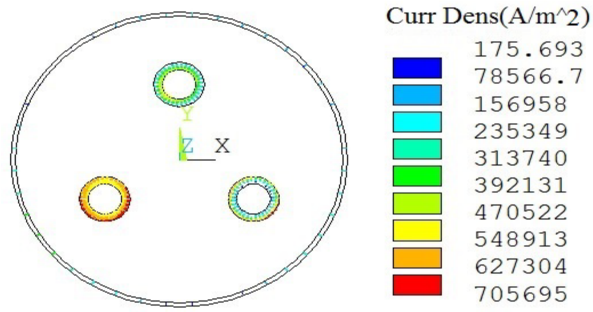

(b) Current density

Fig. 4. Flux density distributions of conductors and tank.

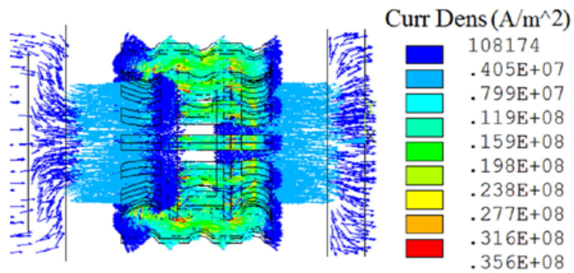

Fig. 5. Currents density distribution of connector.

B. Steady power losses

Steady state power losses of different parts of the three-phase enclosure type GIS bus capsule under different working currents are illustrated in Fig. 6. The increase of working currents can result in larger power losses, leading to a rise in temperature. The power losses of B phase conductor and shield are greater than those in two other phases. The power losses of shield are small compared with tank and bus conductors. The temperature sensors mounted on the tank should have enough precision to measure the temperature change of bus connector, since the power losses of connector are small.

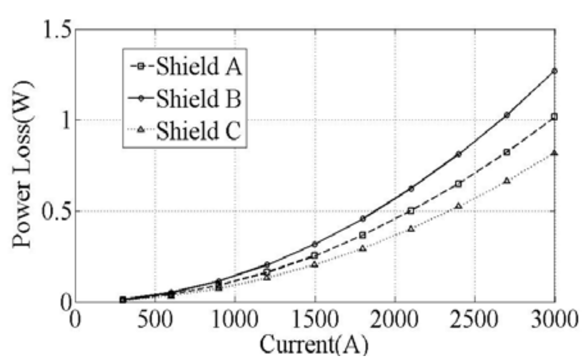

(a) Shield

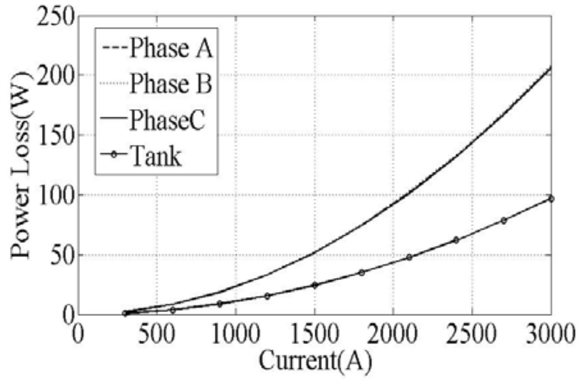

(b) Conductors and tank

Fig. 6. Power losses of different parts as a function of current.

V. SHORT CIRCUIT ELECTROMAGNETIC FORCE ANALYSIS

In this paper, the electromagnetic force under B phase short circuit condition is calculated. The 50-Hz short circuit current with the peak value of 25kA is applied in the B phase conductor. The instantaneous values of short circuit can be represented as follows:

$$\left.\begin{aligned} i_a(t) &= \sqrt{2}I_1\left(\cos\omega t\right) \\ i_b(t) &= \sqrt{2}I_2\left(e^{-\alpha t} - \cos(\omega t - \frac{2}{3}\pi)\right) \\ i_c(t) &= \sqrt{2}I_1\left(\cos(\omega t + \frac{2}{3}\pi)\right) \end{aligned}\right\}, \tag{21}$$

where

I_1=900A, I_2=10kA, ω=100π and a=22.311s^{-1}.

A. Short circuit electromagnetic force of conductor and tank

The electromagnetic forces of buses and tank at short circuit current peak time (6.7 ms) are shown in Fig. 7. It can be seen from nodal force distributions of conductors and tank that electromagnetic force act mainly on B phase conductor and tank under B phase short circuit condition. The electromagnetic forces of B phase conductor and tank in the opposite direction have equal amplitudes.

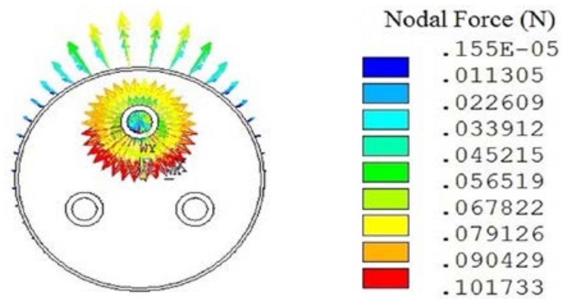

Fig. 7. Electromagnetic forces of bus conductors and tank.

The instantaneous values of short circuit electromagnetic forces in bus conductors and tank is shown in Fig. 8. The short circuit electromagnetic forces consist mainly of 50-Hz and 100-Hz components. The electromagnetic forces at 50-Hz with absolute domination, while the electromagnetic forces at 100-Hz are negligible. Compared with imagine currents method, the electromagnetic force of conductor is slightly smaller due to the interaction between current carriers. Affected by the short-circuit current of b-phase bus conductor, the resultant forces consisting of conductor gravities and electromagnetic forces in bus conductors are large enough to overcome the hold forces exerted by the contact springs; which can cause thermal damage to bus bar joint, due to poor contact. The tank flange joint connection may also be damaged due to the effect of tank short circuit electromagnetic force. So when short circuit fault occurs, all the bus capsules of the GIS equipment where short circuit current flows through, must be checked to make sure that there is no damage at all to the bus conductor connectors and tank flange connections.

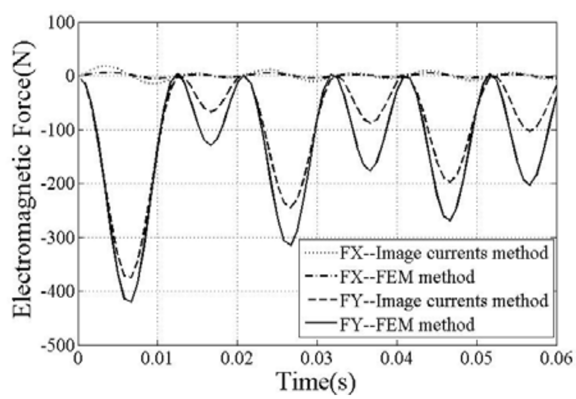

(a) Conductor

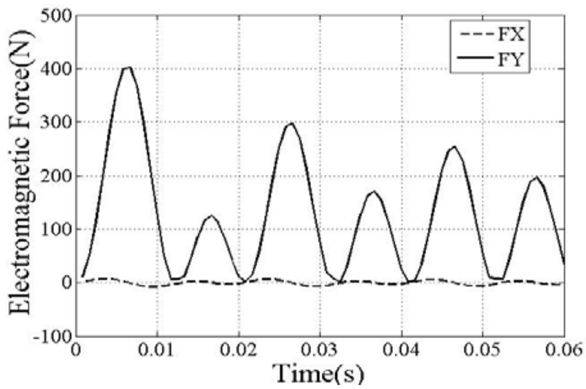

(b) Tank

Fig. 8. Electromagnetic force under B phase short circuit condition.

B. Short circuit electromagnetic force of plug-in connector

The plug-in connector used in GIS bus capsule contains 16 contact fingers, which are arranged around the center conductor axis. In addition to the Holm force and the Lorentz force, plug-in connector electromagnetic forces also include the centrifugal force produced by the current interaction between contact fingers. The total nodal force of plug-in connector under the peak short current is shown in Fig. 9. It can be seen that the resultant electromagnetic force on connector is repulsion force, which can reduce the contact force between finger and bus.

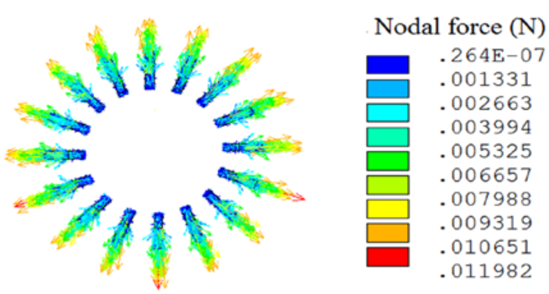

Fig. 9. Electromagnetic forces of plug-in connectors.

The results from different calculation methods compared with 3-D FEM model are shown in Fig. 10. The electromagnetic force by the Holm formula is larger than that from closed-formulas, for the reason that only Holm force in plug-in connector is considered; whereas attractive forces between fingers can produce radial component force in the opposite direction to Holm force. The results calculated by FEM method are larger than that from closed-formulas, because the latter doesn't consider the electric repulsion force produced by the parallel currents between the conductor and fingers. It can be seen from the comparison that the 3-D FEM method can overcome the shortcomings of closed-formulas, which cannot consider the structure of plug-in connectors and has more accurate calculation results.

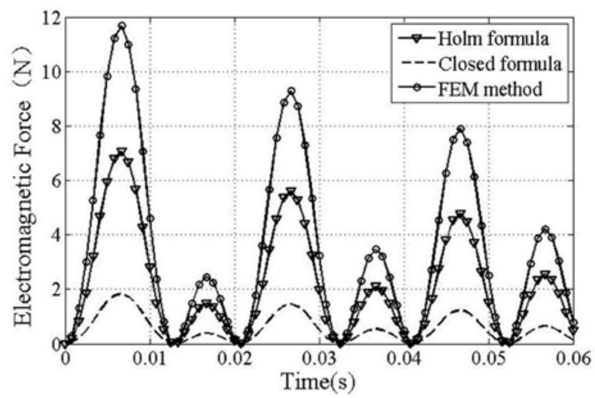

Fig. 10. Electromagnetic force between per contact spot.

According to what is mentioned above, the contact force of per contact spot is about 37N and the peak value of electromagnetic force is up to 12N. Part of the contact force offset by the electromagnetic force under short circuit conditions. Contact resistance and contact temperature will increase due to the decrease of contact force. Relative displacement between connector and bus happens because of the gravity and electro-magnetic force exerted on bus, leading to contact degradation.

VI. CONCLUSION

Steady state power losses and short circuit electromagnetic forces of three phase enclosure type GIS bus capsule is analyzed in this paper. A 3-D finite element model has been developed for the analysis of electromagnetic field and electromagnetic force under normal and single phase short circuit conditions. The calculation results show that under normal conditions the distribution of current density in conductor and tank are not uniform, because of skin effect and proximity effect. The power losses of shield are smaller compared with tank and bus conductors. The short circuit electromagnetic force is large enough to overcome hold forces exerted by the contact springs, which cause bus bar joint thermal damage due to poor contact and the tank flange joint connection may also be damaged due to the effect of short circuit electromagnetic force. The calculation results can be used in optimization designing and condition monitoring of three phase enclosure type GIS.

ACKNOWLEDGEMENT

This work was supported by the Fundamental Research Funds for the China Central Universities (2012207020208).

REFERENCES

[1] A. H. Cookson and C. S. Cleale, "Three-conductor compressed gas cable optimization," *EPRI PROJECT 7840 Final Report*, February 1979.

[2] J. K. Kim and S. C. Hahn, "Temperature rise prediction of EHV GIS bus bar by coupled magneto-thermal finite element method," *IEEE Trans. Magnetics*., vol. 41, no. 5, pp. 1636-1639, 1994.

[3] S. W. Kim, H. H. Kim, and S. C. Hahn, "Coupled finite-element-analytic technique for prediction of temperature rise in power apparatus," *IEEE Trans. Magnetics*., vol. 38, no. 2, pp. 921-924, 2002.

[4] D. Labirdis and V. Hatziathanassiou, "Finite element computation of field, forces and inductances in underground SF_6 insulated cables using a coupled magneto-thermal formulation," *IEEE Trans. Magnetics*., vol. 30, no. 4, pp. 1407-1415, 1994.

[5] H. K. Kim, J. K. Jung, K. Y. Park, C. H. Im, and H. K. Jung, "Efficient technique for 3-D finite element analysis of skin effect in current-carrying conductors," *IEEE Trans. Magnetics*., vol. 40, no. 2, pp. 1326-1329, 2004.

[6] C. T. Liu and S. Y. Yao, "Electromagnetic field and force analyses of a noncontacting conveyance system for steel mill application," *IEEE Trans. Magnetics*., vol. 38, no. 5, pp. 3318-3320, 2002.

[7] T. Bauer, W. Mai, and G. Henneberger, "Improved 3D coupled calculations of the structural-dynamic behavior of induction furnaces excited by electromagnetic forces using adaptive algorithms," *IEEE Trans. Magnetics*., vol. 36, no. 4, pp. 1565-1568, 2000.

[8] P. Pellerey, V. Lanfranchi, and G. Friedrich, "Coupled numerical simulation between electromagnetic and structural models, influence of the supply harmonics for synchronous machine vibrations," *IEEE Trans. Magnetics*., vol. 48, no. 2, pp. 983-986, 2012.

[9] I. Shokichi, T. Yoshiaki, K. Yoshihiro, and O. Tomohiro, "Numerical analysis of electromagnetic forces in low voltage ac circuit breakers using 3-D finite element method taking into account eddy currents," *IEEE Trans. Magnetics*., vol. 34, no. 5, pp. 2597-2600, 1998.

[10] H. Hama, T. Marutani, K. Takatsuka, T. Nitta, and T. Tanabe, "Characteristics of short circuit electromagnetic forces in three phase enclosure type gas insulated bus," *IEEE Trans. Power Delivery*, vol. PWRD-2, no. 2, pp. 367-373, 1987.

[11] Y. Kanno, T. Amemiya, N. Takahashi, and N. Kobayahi, "The short circuit electro-magnetic force of the three-phase encapsulated gas insulated bus-bar," *IEEE Trans. Power Apparatus and Systems*, vol. PAS-103, no. 6, pp. 1386-1393, 1984.

[12] S. Mon, S. Imai, K. Ninomiya, H. Hata, K. Itaka, and T. Hara, "Characteristics of gas insulated transmission lines bonded at both ends in relation to short-circuit force," *IEEE Trans. Power Apparatus and Systems*, vol. PAS-100, no. 5, pp. 2311-2319, 1981.

[13] T. Takeuchi, T. Yoshizawa, and Y. Kuse, "3-D nonlinear transient electromagnetic analysis of short circuit electromagnetic forces in a three-phase enclosure-type gas insulated bus," *IEEE Trans. Magnetics*, vol. 36, no. 4, pp. 1754-1757, 2000.

[14] K. Yoshihiro, M. Hiroyuki, and I. Shokichi, "3-D finite element analysis of electro-dynamic repulsion forces in stationary electric contacts taking into account asymmetric shape," *IEEE Trans. Magnetics*, vol. 33, no. 2, pp. 1994-1999, 1997.

[15] A. E. Emanuel, H. C. Doepken, and P. C. Bolin, "Design and test of a sliding plug-in conductor connector for compressed gas-insulated cables," *IEEE Trans. Power Apparatus and Systems*, vol. 95, no. 2, pp. 570-579, 1976.

[16] R. Holm, "Electric contacts, theory and applications," *Springer*, New York, 1979.

Xiangyu Guan is a Ph.D. student at Electrical Engineering College, Wuhan University. His research interests mainly focus on numerical methods of field calculation and condition monitoring of electrical equipment.

Naiqiu Shu is a Professor at Electrical Engineering College, Wuhan University. He received his M.S. and Ph.D. degrees at Electrical Engineering College, Wuhan University. He research interests mainly focus on condition monitoring of electrical equipment.